



NLR-TP-99295

Resolving the dependence on free-stream values for the k-omega turbulence model

J.C. Kok



NLR-TP-99295

Resolving the dependence on free-stream values for the k-omega turbulence model

J.C. Kok

This report is based on an article submitted to the AIAA Journal.

The contents of this report may be cited on condition that full credit is given to NLR and the author.

| | |
|--------------------------|----------------|
| Division: | Fluid Dynamics |
| Issued: | July 1999 |
| Classification of title: | unclassified |



Summary

In this paper, the dependency of the $k-\omega$ eddy-viscosity turbulence model on free-stream values is analyzed by considering a one-dimensional, unsteady model problem for turbulent/non-turbulent interfaces. Constraints on the diffusion coefficients of the $k-\omega$ model are derived for which a particular weak solution exists, representing a turbulent front moving forward into a non-turbulent region. The standard values of the diffusion coefficients in the Wilcox $k-\omega$ model, which suffers from the free-stream dependency, violate these constraints. It is demonstrated that a new set of diffusion coefficients that satisfies the constraints, resolves the free-stream dependency at low free-stream eddy-viscosity levels for a flat-plate constant-pressure boundary layer and the RAE2822 airfoil, while maintaining the correct near-wall solution.



Contents

| | |
|---------------------------|----|
| List of symbols | 5 |
| List of figures | 6 |
| 1 Introduction | 7 |
| 2 Analysis | 9 |
| 3 Results | 12 |
| 4 Conclusions | 14 |
| 5 Acknowledgements | 15 |
| 6 References | 16 |

4 Figures

(20 pages in total)



List of symbols

| | |
|-------------------------------------|---|
| c | velocity of turbulent/non-turbulent front |
| C_D | cross-diffusion term |
| C_p | pressure coefficient |
| C_f | skin-friction coefficient |
| k | turbulent kinetic energy |
| M | Mach number |
| P_k, P_ω | production terms of k and ω |
| Re | Reynolds number |
| Re_t | turbulent Reynolds number |
| t | time |
| \vec{u}, u_i, \mathbf{u} | velocity vector with Cartesian components |
| \vec{x}, x_i, \mathbf{y} | position vector with Cartesian components |
| α | angle of attack |
| α_ω | coefficient of production term of ω |
| β^*, β | coefficients of dissipation terms of k and ω |
| δ_0 | length scale of weak solution of model problem |
| ϵ | turbulent dissipation rate |
| κ | Von Kármán constant |
| μ, μ_t | dynamic molecular and eddy viscosity coefficients |
| ν_t | kinematic eddy viscosity coefficient |
| ρ | density |
| $\sigma_k, \sigma_\omega, \sigma_d$ | coefficients of diffusion terms of k and ω |
| τ^R, τ_{ij}^R | Reynolds-stress tensor with Cartesian components |
| ω | specific turbulent dissipation rate |

Subscripts and superscripts:

| | |
|----------|--|
| 0 | constant of weak solution of model problem |
| + | law-of-the-wall scaling |
| ∞ | free-stream value |



List of figures

- Figure 1 Skin-friction coefficient (C_f) for flat plate with k - ω model ($Re_\infty = 10^7$, $M_\infty = 0.5$, $Re_{t,\infty} = 10^{-2}$, $k_\infty/u_\infty^2 = \text{tkinf}$). 17
- Figure 2 Velocity distribution (law-of-the-wall scaling) for flat plate with k - ω model ($Re_x = 5 \cdot 10^6$, $M_\infty = 0.5$, $Re_{t,\infty} = 10^{-2}$, $k_\infty/u_\infty^2 = \text{tkinf}$). 18
- Figure 3 Eddy-viscosity distribution (law-of-the-wall scaling) for flat plate with k - ω model ($Re_x = 5 \cdot 10^6$, $M_\infty = 0.5$, $Re_{t,\infty} = 10^{-2}$, $k_\infty/u_\infty^2 = \text{tkinf}$). 19
- Figure 4 Pressure and skin-friction distribution for RAE2822 airfoil, case 9 with k - ω model ($M_\infty = 0.73$, $Re_\infty = 6.5 \cdot 10^6$, $\alpha = 2.8^\circ$, $Re_{t,\infty} = 10^{-2}$, $k_\infty/u_\infty^2 = 10^{-6}$). 20

1 Introduction

The $k-\omega$ two-equation eddy-viscosity model has become a widely used turbulence model for wall-bounded, aerodynamic flows for two main reasons: it does not require any wall-damping functions nor the computation of wall distances, and it is less stiff than $k-\epsilon$ models in the near-wall region. In particular the first property is desirable for complex configurations. However, the original $k-\omega$ model of Wilcox (Ref. 1, 2) has one main drawback: the results depend on the free-stream value of the turbulence variables (in particular ω) even at very low free-stream eddy-viscosity levels. This free-stream dependence seems to be the strongest for free shear layers, but is also significant for boundary layers. As shown by Menter (Ref. 3), a correct solution for boundary layers can be obtained if a sufficiently large value of ω is applied at the boundary-layer edge. In practice, however, it is difficult to obtain such a large value at the boundary-layer edge, because the turbulence variables are generally prescribed at a far-field boundary and will decay in the free stream.

Since the $k-\epsilon$ model generally does not seem to have this free-stream dependency, Menter (Ref. 4) proposed to resolve the free-stream dependency by a blending between the standard Wilcox model and the standard $k-\epsilon$ model (in a $k-\omega$ formulation), such that the model switches from $k-\omega$ to $k-\epsilon$ approaching the boundary-layer edge. The main effect of switching to the $k-\epsilon$ model is the inclusion of an extra term (the so-called cross-diffusion term) in the ω equation. This model, however, requires the wall distance to evaluate the blending function, thus losing one of the advantages of the $k-\omega$ model. Wilcox (Ref. 5) proposed to include the cross-diffusion term without any blending functions, and to switch it off when it becomes negative, so that it is not effective in the near-wall region, which is crucial for a correct behaviour of the $k-\omega$ model. The analysis and results in this paper, however, will show that with the model coefficients chosen by Wilcox, this model does not effectively resolve the free-stream dependency.

An alternative approach is to enforce the correct (large) value of ω at the boundary-layer edge. For example, in the $k-g$ model of Kalitzin et al. (Ref. 6) (with $g = 1/\sqrt{\omega}$) this is done by switching off the production (and dissipation) terms of g in non-turbulent regions. Also a background production of k and ω could be used as suggested by De Cock (Ref. 7). However, the large value of ω may have the undesired effect that laminar/turbulent transition is suppressed at specified transition lines.

Recently, Wilcox (Ref. 2) has defined a new version of the $k-\omega$ model in which the cross-diffusion term is not added to the ω equation, but is used to modify the coefficient of the dissipation term in the k equation. This modification has been tuned such that the spreading rates for the similarity



solutions of several free-shear flows are as close as possible to experimental values for the limiting case that the free-stream values of k and ω approach zero. No attempt has been made to make the spreading rates independent from the free-stream values (in fact they are not), but in practice the free-stream dependency is less problematic, since the correct solution is obtained for a sufficiently small (instead of sufficiently large) free-stream value of ω .

The behaviour of the $k-\epsilon$ type models at free-stream edges of turbulent regions was studied by Cazalbou et al. (Ref. 8). A one-dimensional model problem, consisting of a set of diffusion equations, was considered together with a particular, weak solution representing a front between a turbulent and a non-turbulent region. Constraints were derived for which the weak solution is valid. The constraints also imply that the front moves into the non-turbulent region. It was demonstrated that most $k-\epsilon$ models show the weak solution, also in practical situations, and that for such weak solutions, the free-stream dependency is weak.

In this paper, the analysis of Cazalbou et al. is extended to the $k-\omega$ model including the cross-diffusion term. Constraints are derived for which a similar weak solution as for the $k-\epsilon$ model exists for the $k-\omega$ model. A new set of values for the diffusion coefficients is defined that satisfies these constraints. It is shown that the free-stream dependency is effectively resolved at low free-stream eddy-viscosity levels for a zero pressure-gradient flat-plate boundary layer and for the RAE2822 airfoil.

All computations have been performed with the NLR flow-simulation system ENFLOW for multi-block structured grids (Ref. 9). The equations are discretized by a cell-centred, finite-volume scheme, using central differencing with matrix artificial dissipation (blending of 2nd- and 4th-order differences with the Jameson pressure switch for the basic flow equations and with a TVD switch for the turbulence-model equations). The basic flow and turbulence-model equations are solved as one system of equations by a multi-grid scheme, using Runge-Kutta time integration, local time stepping, and implicit residual averaging.



2 Analysis

The k - ω model equations, including the cross-diffusion term, are given by

$$\frac{\partial \rho k}{\partial t} + \frac{\partial(\rho k u_j)}{\partial x_j} = P_k - \beta^* \rho \omega k + \frac{\partial}{\partial x_j} \left((\mu + \sigma_k \mu_t) \frac{\partial k}{\partial x_j} \right), \quad (1)$$

$$\frac{\partial \rho \omega}{\partial t} + \frac{\partial(\rho \omega u_j)}{\partial x_j} = P_\omega - \beta \rho \omega^2 + \frac{\partial}{\partial x_j} \left((\mu + \sigma_\omega \mu_t) \frac{\partial \omega}{\partial x_j} \right) + C_D, \quad (2)$$

with ρ the density, \vec{u} the velocity vector, μ the molecular-viscosity coefficient, k the turbulent kinetic energy, ω the specific turbulent dissipation, and $\mu_t = \rho k / \omega$ the eddy-viscosity coefficient.

The production and cross-diffusion terms are given by

$$P_k = \tau_{ij}^R \frac{\partial u_j}{\partial x_i}, \quad (3)$$

$$P_\omega = \frac{\alpha_\omega \omega}{k} P_k, \quad (4)$$

$$C_D = \sigma_d \frac{\rho}{\omega} \max \left\{ \frac{\partial k}{\partial x_i} \frac{\partial \omega}{\partial x_i}, 0 \right\}, \quad (5)$$

with τ^R the Reynolds-stress tensor.

The k - ω model has six closure coefficients: α_ω , β^* , β , σ_k , σ_ω , and σ_d . Following Wilcox (Ref. 1), four relations between these coefficients can be derived. First, to be consistent with the experimental decay of the turbulent kinetic energy for homogeneous, isotropic turbulence, $\beta^*/\beta = 6/5$. Second, to obtain the correct solution in the inner layer of a constant-pressure boundary layer, consistent with the law of the wall, $\alpha_\omega = \beta/\beta^* - \sigma_\omega \kappa^2 / \sqrt{\beta^*}$ (with $\kappa = 0.41$ the Von Kármán constant), and $\beta^* = 0.09$, while further, $\sigma_\omega = 0.5$ or otherwise a low-Reynolds-number modification is needed (Ref. 5). The effect of the two remaining coefficients, σ_k and σ_d , on the solution in the inner layer is weak; they will be tuned to obtain a desirable behaviour of the model at the boundary-layer edge.

Consider the following set of 1D diffusion equations as a model for free-stream edges of turbulent regions:

$$\frac{\partial k}{\partial t} = \frac{\partial}{\partial y} \left(\sigma_k \nu_t \frac{\partial k}{\partial y} \right), \quad (6)$$

$$\frac{\partial \omega}{\partial t} = \frac{\partial}{\partial y} \left(\sigma_\omega \nu_t \frac{\partial \omega}{\partial y} \right) + \sigma_d \frac{1}{\omega} \frac{\partial k}{\partial y} \frac{\partial \omega}{\partial y}, \quad (7)$$

$$\frac{\partial u}{\partial t} = \frac{\partial}{\partial y} \left(\nu_t \frac{\partial u}{\partial y} \right), \quad (8)$$



with $\nu_t = k/\omega$ and with the diffusion coefficients $\sigma_k, \sigma_\omega > 0$ and $\sigma_d \geq 0$. This set of equations has a particular weak solution, consisting of a front between a turbulent and a non-turbulent region moving with a velocity c in the positive y direction,

$$k = k_0 f^{\sigma_\omega / (\sigma_\omega - \sigma_k + \sigma_d)}, \quad (9)$$

$$\omega = \omega_0 f^{(\sigma_k - \sigma_d) / (\sigma_\omega - \sigma_k + \sigma_d)}, \quad (10)$$

$$u = u_0 f^{\sigma_k \sigma_\omega / (\sigma_\omega - \sigma_k + \sigma_d)}, \quad (11)$$

$$\nu_t = \nu_0 f, \quad (12)$$

with

$$f = \max \left\{ \frac{ct - y}{\delta_0}, 0 \right\}, \quad (13)$$

$$c = \frac{\nu_0}{\delta_0} \frac{\sigma_k \sigma_\omega}{\sigma_\omega - \sigma_k + \sigma_d}, \quad (14)$$

$$\nu_0 = \frac{k_0}{\omega_0}, \quad (15)$$

and with k_0, ω_0 , and δ_0 positive constants. (For $y > ct$, $\omega = 0$ is not a strict solution of the equations; in practice, small non-zero values for k and ω are used in the free stream.)

A number of constraints can be derived from this particular solution. First, for this solution to be a valid weak solution of the model problem, the three transported variables (k , ω , and u) must go to zero when approaching the front from the side $y < ct$, resulting in the constraints

$$\sigma_\omega - \sigma_k + \sigma_d > 0, \quad (16)$$

$$\sigma_k - \sigma_d > 0. \quad (17)$$

Second, the slope of u at the front is required to be finite (physically valid), resulting in

$$\sigma_\omega - \sigma_k + \sigma_d \leq \sigma_k \sigma_\omega. \quad (18)$$

Note that constraint (17) ensures that the slope of k at the front is also finite. Third, for the particular solution of the model problem to be representative for the solution of the k - ω model at a boundary-layer edge, we require the production and dissipation terms in the k and ω equations to be negligible compared to the diffusion terms when approaching the front. For the k equation,

the diffusion, production, and dissipation terms are

$$\frac{\partial}{\partial y} \left(\sigma_k \nu_t \frac{\partial k}{\partial y} \right) \sim f^{(\sigma_k - \sigma_d)/(\sigma_\omega - \sigma_k + \sigma_d)}, \quad (19)$$

$$\nu_t \left(\frac{\partial u}{\partial y} \right)^2 \sim f^{((2\sigma_k - 1)\sigma_\omega + \sigma_k - \sigma_d)/(\sigma_\omega - \sigma_k + \sigma_d)}, \quad (20)$$

$$\beta^* k \omega \sim f^{(\sigma_\omega + \sigma_k - \sigma_d)/(\sigma_\omega - \sigma_k + \sigma_d)}. \quad (21)$$

Requiring the power of f in the production and dissipation terms to be larger than the power of f in the diffusion term, one obtains the constraints

$$\sigma_k > 0.5, \quad (22)$$

$$\sigma_\omega > 0. \quad (23)$$

For the ω equation, the same constraints are obtained.

An important consequence of constraint (16) is that the velocity of the front is positive ($c > 0$). Thus, the front moves into the non-turbulent region. On this basis, one may expect the dependence of the solution on the free-stream values of k and ω to be weak (if the free-stream eddy viscosity is negligibly small).

The standard Wilcox model ($\sigma_\omega = 0.5, \sigma_k = 0.5, \sigma_d = 0$) as well as the Wilcox model including cross diffusion ($\sigma_\omega = 0.6, \sigma_k = 1.0, \sigma_d = 0.3$) do not satisfy constraint (16). For the Menter baseline model, the set of coefficients obtained near the boundary-layer edge ($\mathcal{Q} = 0.856, \sigma_k = 1.0, \sigma_d = 2\sigma_\omega$) satisfies constraint (16), resulting in a positive velocity of the front, but not constraint (17), so that the weak solution is not strictly valid (ω goes to infinity when approaching the front).

The following new choice of values for the diffusion coefficients, denoted as the TNT set,

$$\sigma_\omega = 0.5, \quad \sigma_k = 2/3, \quad \sigma_d = 0.5 \quad (24)$$

satisfies all formulated constraints of the turbulent/non-turbulent (TNT) analysis above. Note that $\sigma_\omega = 0.5$, so that near-wall modifications (either low-Reynolds modifications or a blending as in the Menter model) are not needed.



3 Results

As a first test case, the flat-plate boundary layer is considered with $Re_\infty = 10^7$ and $M_\infty = 0.5$. Transition is prescribed at 5% from the leading edge. Three variants of the $k-\omega$ model are used: standard Wilcox, Wilcox including cross diffusion, and the present TNT choice. For all three models, the free-stream turbulent Reynolds number is kept constant to $Re_{t,\infty} = (\mu_t/\mu)_\infty = 10^{-2}$, while the free-stream value of k is varied by several orders of magnitude ($k_\infty/u_\infty^2 = 10^{-6}, 10^{-8}, 10^{-10}$), thus also varying the free-stream value of ω . A grid is used with 64×64 grid cells of which 40 in stream direction on the flat plate and approximately 30 to 40 in normal direction inside the turbulent boundary layer. For the first grid point above the flat plate $y^+ \approx 1$.

Figures 1 to 3 show the computed skin-friction coefficients, compared to the skin-friction law given by Cebeci and Smith (Ref. 10) (equation (5.4.23)), as well as the velocity and eddy-viscosity distributions at the location $Re_x = 5 \cdot 10^6$.

For the standard Wilcox model the dependency of the solution on the free-stream values is apparent. This dependency is most clearly revealed for the eddy-viscosity distribution (Fig. 3a). The transport of low free-stream values of ω into the boundary layer results in a net production of eddy viscosity near the boundary-layer edge, which becomes stronger as the free-stream value of ω is decreased. The larger eddy-viscosity levels cause an increase of the skin-friction coefficient (Fig. 1a). To obtain the correct solution, the value of ω at the boundary-layer edge should be sufficiently large as pointed out by Menter (Ref. 3). In practice, this value is not obtained (even for the largest value of k_∞) because the value of ω has decayed before the boundary-layer edge is reached. As a consequence, the skin-friction distribution lies above the theoretical law.

The Wilcox model with cross diffusion also shows the free-stream dependency, although less pronounced than the standard Wilcox model. Furthermore, the velocity profile deviates from the log law (Fig. 2b), because $\sigma_\omega \neq 0.5$ and no low-Reynolds-number correction has been included. This also explains why the skin-friction distribution lies significantly above the theoretical law (Fig. 1b).

Consistent with the analysis, the computations with the TNT choice of diffusion coefficients show practically no free-stream dependency. Although the distribution of the eddy viscosity at the boundary-layer edge is still slightly free-stream dependent (Fig. 3c), the *level* of eddy viscosity and therefore also the skin-friction coefficient are not. Furthermore, the velocity distribution is consistent with the log law (Fig. 2c).

Finally, to ensure that the conclusions are not disturbed by numerical errors, the grid convergence of the solution has been checked. Figures 1d, 2d, and 3d show that for the TNT $k-\omega$ variant, the fine-grid results are sufficiently grid converged (apart from the transition region).

As a second test case, the RAE2822 airfoil is considered at $M_\infty = 0.73$ and with $Re_\infty = 6.5 \cdot 10^6$ and $\alpha = 2.8^\circ$ (case 9 of reference 11). Transition is fixed at 3% from the leading edge. The same three variants of the $k-\omega$ model are used, as well as the Cebeci–Smith model for reference. For the $k-\omega$ models, $Re_{t,\infty} = 10^{-2}$ and $k_\infty/u_\infty^2 = 10^{-6}$. A C-type grid is used with 528×96 grid cells, of which 384 around the airfoil and approximately 30 to 40 in normal direction inside the turbulent boundary layer. For the first grid point above the solid wall $y^+ < 1$. The far field is located at 50 chords from the airfoil.

Figure 4 compares the pressure and skin-friction distributions of the different models to the experimental results. For the two Wilcox variants, the shock is located slightly aft compared to the Cebeci–Smith model and the new $k-\omega$ variant. Similarly as for the flat plate, the TNT $k-\omega$ variant gives lower levels of the skin friction than the two Wilcox variants, and in this case closer to the Cebeci–Smith model and to the experimental values. Most likely, the more aft shock position and the higher skin friction for the two Wilcox variants are a result of higher eddy-viscosity levels (as were seen for the flat plate). This again may be a consequence of the values of ω at the boundary-layer edge being too low.

For the TNT $k-\omega$ variant, the absence of free-stream dependency is shown in figure 4c for the skin-friction coefficient. In figure 4d, also the grid dependency is checked.



4 Conclusions

The solutions of the standard Wilcox $k-\omega$ model are dependent on the free-stream values of the turbulence variables, even at low free-stream eddy-viscosity levels. When the so-called cross-diffusion term is included in the equation for ω (when positive), the $k-\omega$ model becomes formally equivalent to the $k-\epsilon$ type models near free-stream edges of turbulent regions. Since most $k-\epsilon$ models do not suffer from free-stream dependency, there seems to be no reason why the $k-\omega$ model including cross-diffusion should. In fact, the theoretical analysis of turbulent/non-turbulent (TNT) interfaces presented in this paper has resulted in a set of constraints which the diffusion coefficients of the $k-\omega$ model should satisfy to resolve the free-stream dependency for a model problem. A new set of diffusion coefficients has been chosen that satisfies this set of constraints. Furthermore, these TNT coefficients allow the correct near-wall solution for a constant-pressure boundary layer without the introduction of any blending functions or near-wall modifications, i.e. without introducing the wall distance. Computations for a flat-plate constant-pressure boundary layer and for a 2D airfoil have demonstrated the effective elimination of the free-stream dependency at low free-stream eddy-viscosity levels with the TNT set of coefficients, while maintaining the correct near-wall solution.



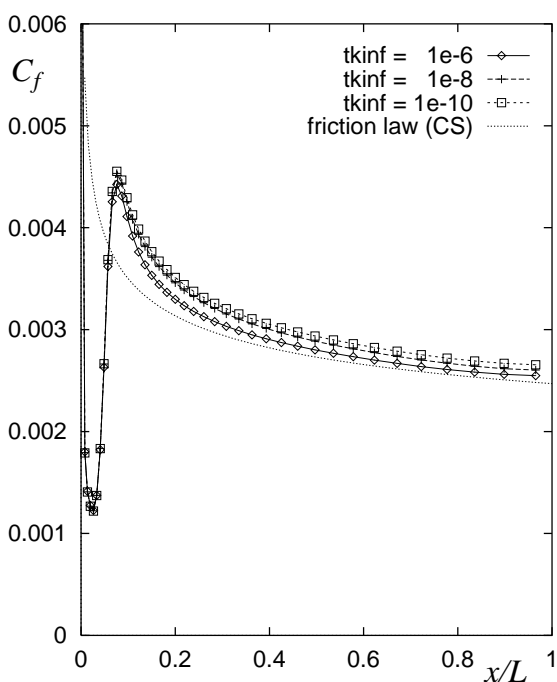
5 Acknowledgements

The ENFLOW system, including the implementation of the $k-\omega$ model, has been developed under a contract awarded by the Netherlands Agency for Aerospace Programmes, contract number 01105N. To some extent the analysis presented here has been carried out within the framework of the AVTAC project. The AVTAC project (Advanced Viscous Flow Simulation Tools for Complete Civil Transport Aircraft Design) is a collaboration between British Aerospace, DASA, CASA, Dassault Aviation, SAAB, Alenia, DLR, ONERA, CIRA, FFA, and NLR. The project is managed by British Aerospace and is funded by the CEC under the IMT initiative (Project Ref: BRPR CT97-0555).

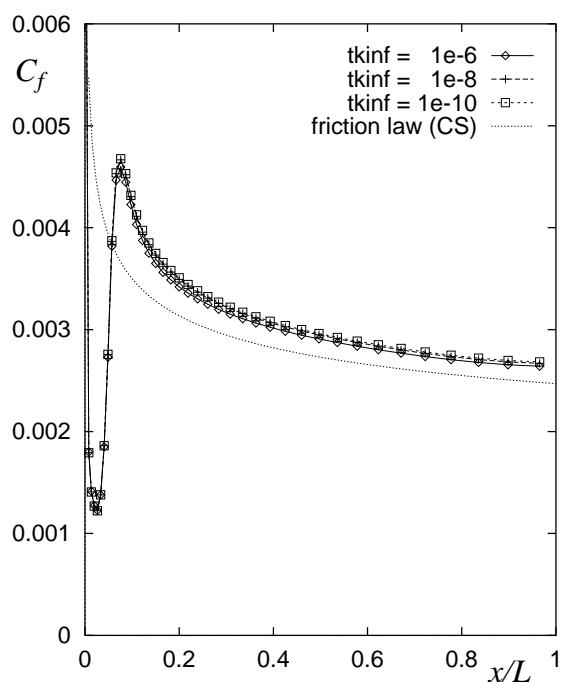


6 References

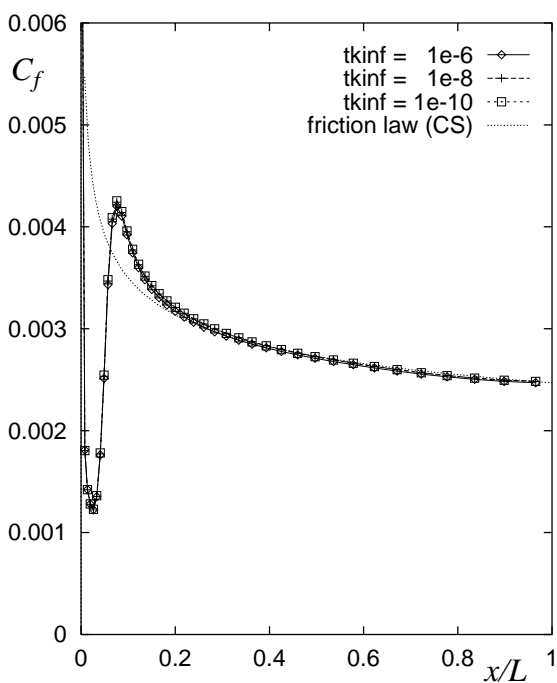
1. Wilcox, D.C., 'Reassessment of the scale-determining equation for advanced turbulence models', *AIAA Journal*, Vol. 26, No. 11, 1988, pp. 1299–1310.
2. Wilcox, D.C., *Turbulence Modeling for CFD*, 2nd ed., DCW Industries, Inc., La Cañada, California, 1998.
3. Menter, F.R., 'Influence of freestream values on $k-\omega$ turbulence model predictions', *AIAA Journal*, Vol. 30, No. 16, 1991, pp. 1657–1659.
4. Menter, F.R., 'Zonal two equation $k-\omega$ turbulence models for aerodynamic flows', AIAA Paper 93-2906, 1993.
5. Wilcox, D.C., 'A two-equation turbulence model for wall-bounded and free-shear flows', AIAA Paper 93-2905, 1993.
6. Kalitzin, G., Gould, A.R.B., and Benton, J.J., 'Application of two-equation turbulence models in aircraft design', AIAA Paper 96-0327, 1996.
7. Cock, K.M.J. de, 'Fully automatic Navier-Stokes algorithm for 2D high-lift flows', *Fifteenth International Conference on Numerical Methods in Fluid Dynamics*, Monterey, California, June 24-28 1996, (NLR TP 96487 U).
8. Cazalbou, J.B., Spalart, P.R., and Bradshaw, P., 'On the behaviour of two-equation models at the edge of a turbulent region', *Physics of Fluids*, Vol. 6, No. 5, 1994, pp. 1797–1804.
9. Boerstoel, J.W., Kassies, A., Kok, J.C., and Spekreijse, S.P., 'ENFLOW, a full-functionality system of CFD codes for industrial Euler/Navier-Stokes flow computations', NLR TP 96286 U, 1996.
10. Cebeci, T. and Smith, A.M.O., *Analysis of Turbulent Boundary Layers*, Academic Press, New York, 1974.
11. Cook, P., McDonald, M., and Firmin, M., 'Airfoil RAE 2822 — pressure distributions and boundary layer wake measurements', AGARD AR 138, 1979.



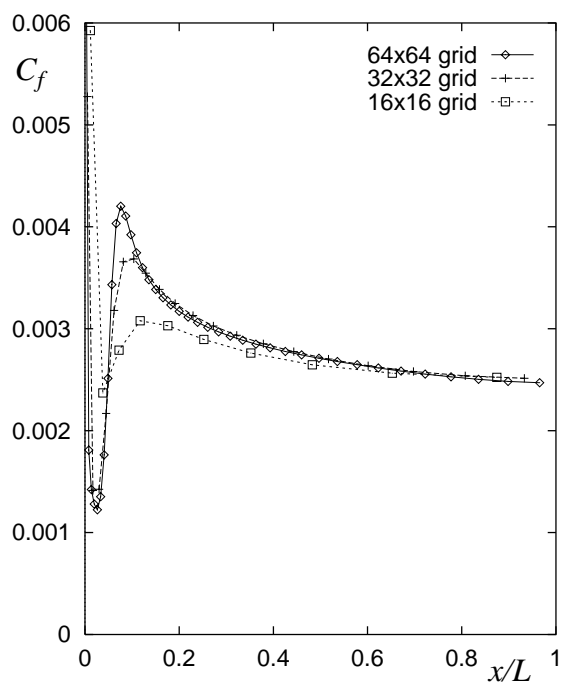
a) Standard Wilcox $k-\omega$ model



b) Wilcox model with cross-diffusion

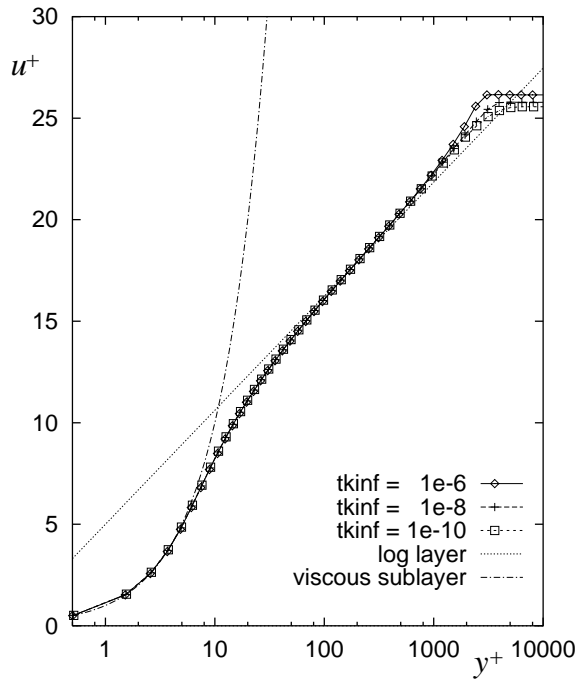


c) TNT variant of $k-\omega$ model

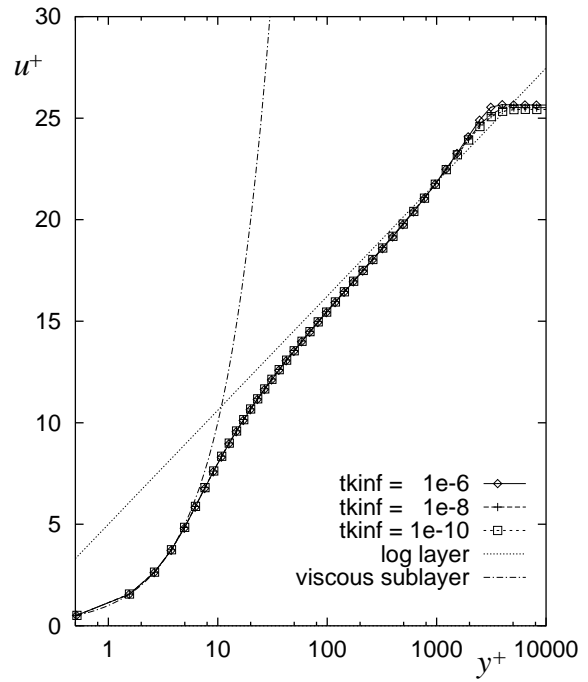


d) Grid dependency of TNT $k-\omega$ variant

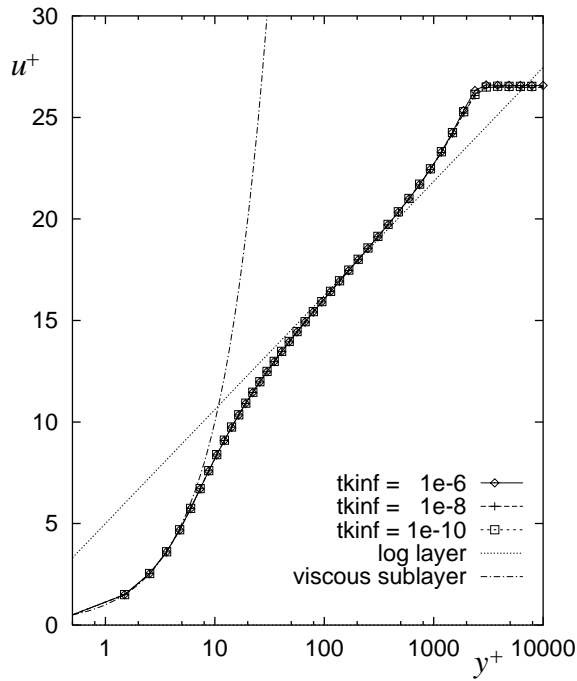
Fig. 1 Skin-friction coefficient (C_f) for flat plate with $k-\omega$ model ($Re_\infty = 10^7$, $M_\infty = 0.5$, $Re_{t,\infty} = 10^{-2}$, $k_\infty/u_\infty^2 = \text{tkinf}$).



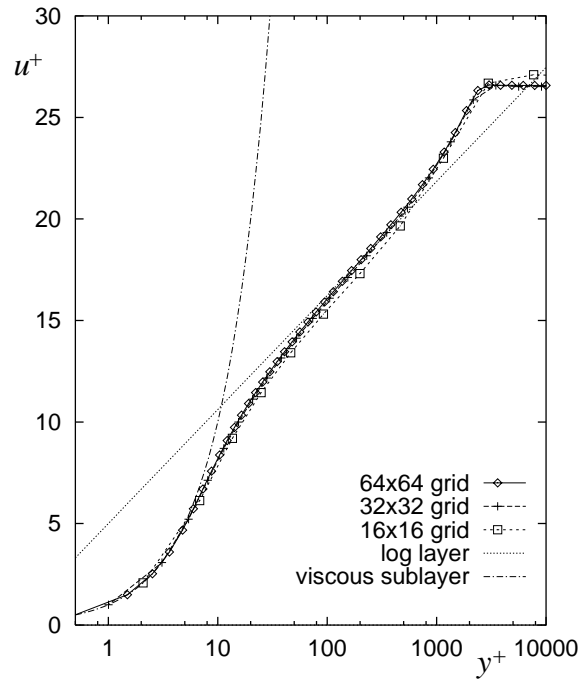
a) Standard Wilcox $k-\omega$ model



b) Wilcox model with cross-diffusion



c) TNT variant of $k-\omega$ model



d) Grid dependency of TNT $k-\omega$ variant

Fig. 2 Velocity distribution (law-of-the-wall scaling) for flat plate with $k-\omega$ model ($Re_x = 5 \cdot 10^6$, $M_\infty = 0.5$, $Re_{t,\infty} = 10^{-2}$, $k_\infty/u_\infty^2 = tkinf$).

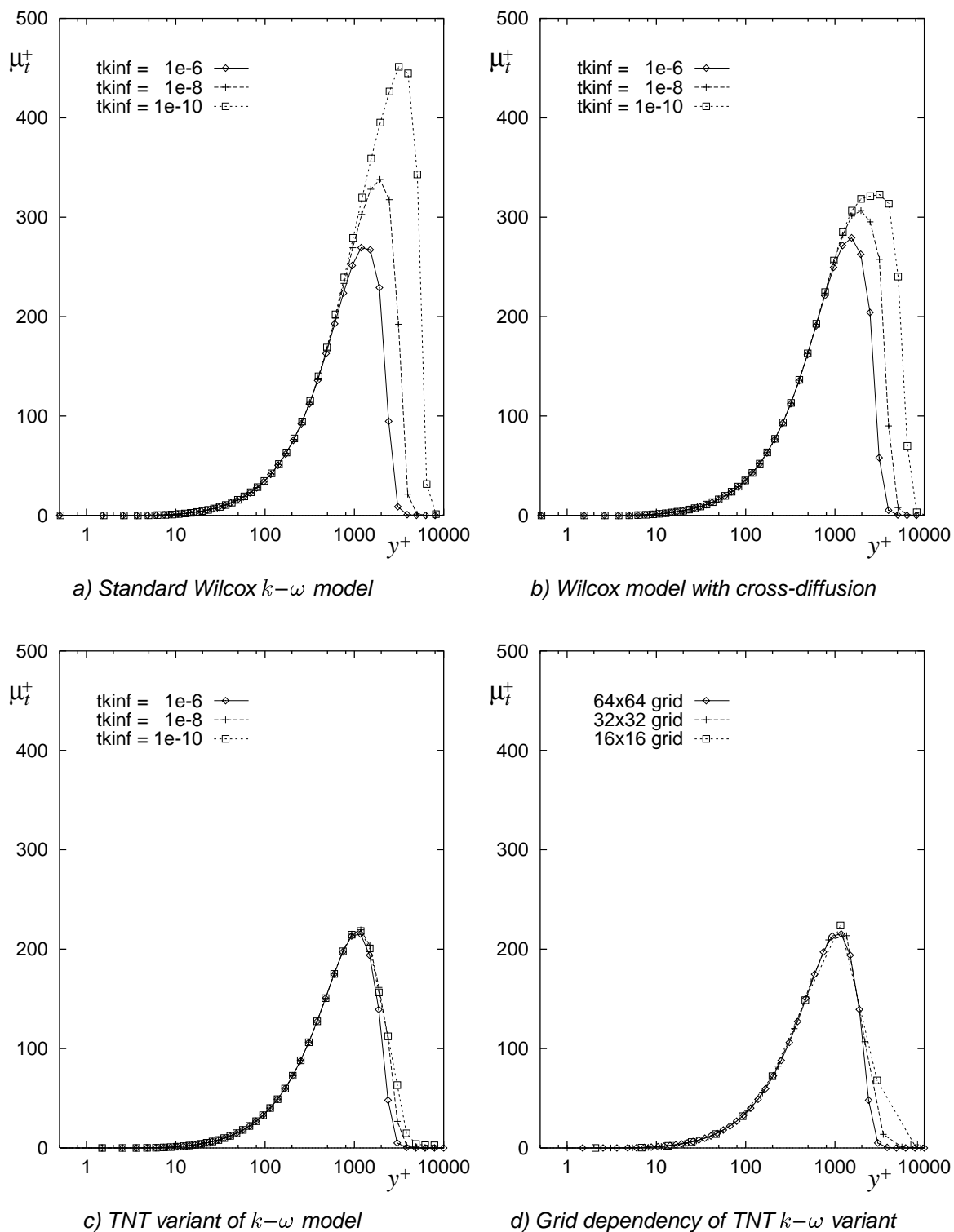
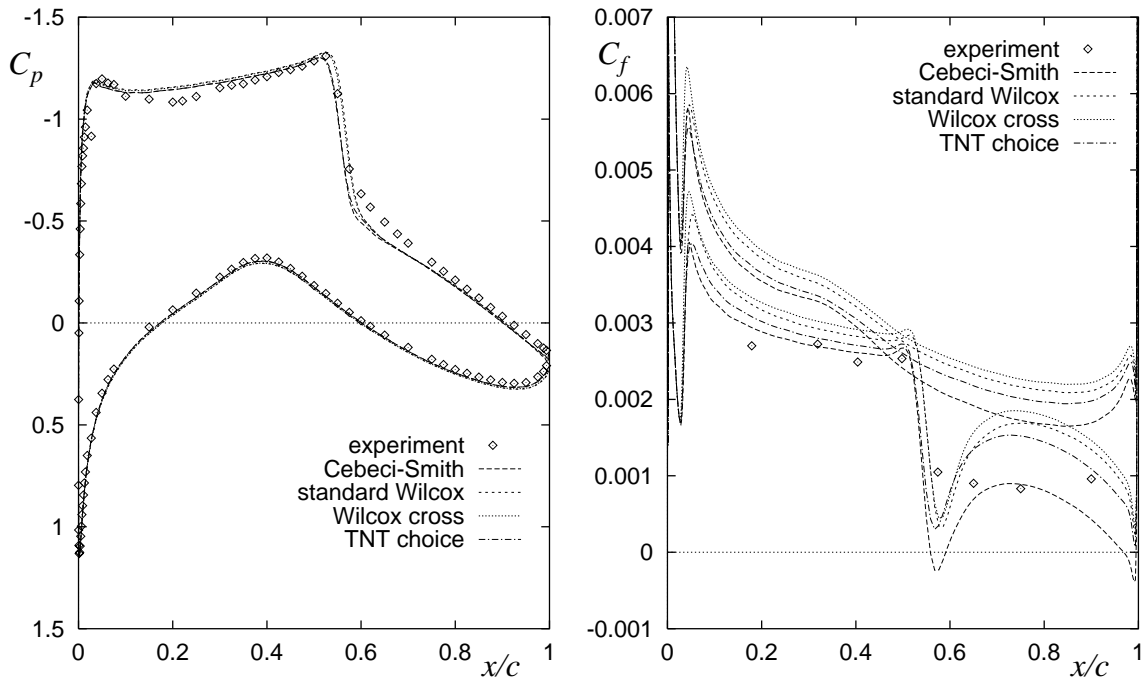
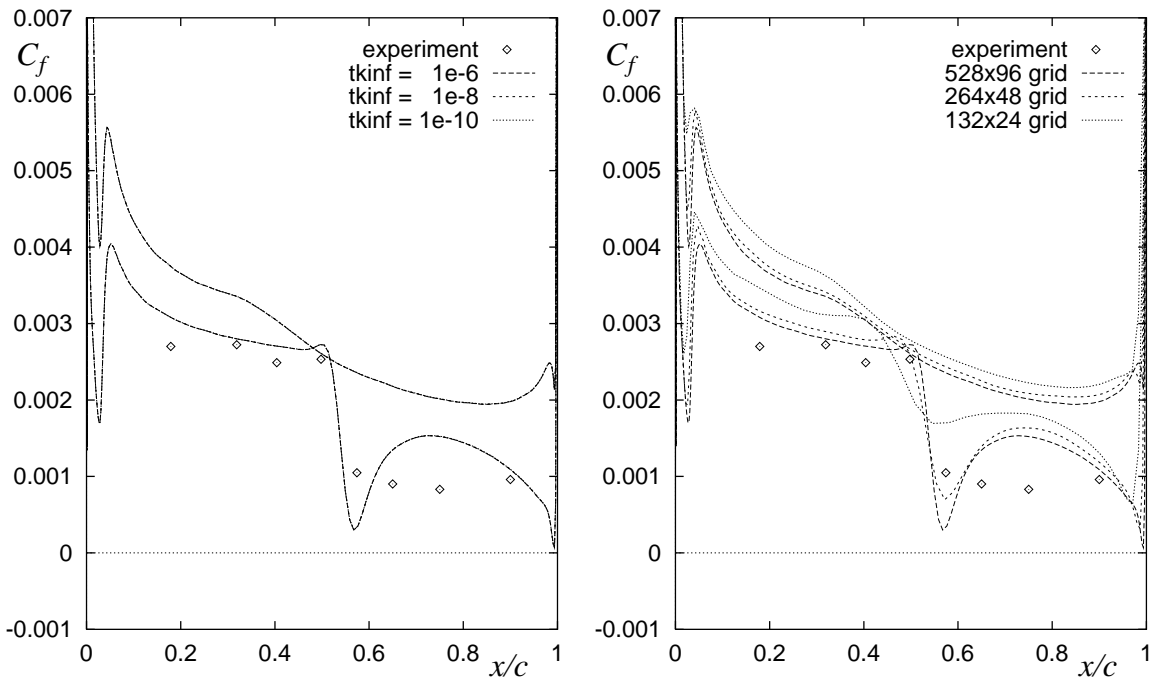


Fig. 3 Eddy-viscosity distribution (law-of-the-wall scaling) for flat plate with $k-\omega$ model ($Re_x = 5 \cdot 10^6$, $M_\infty = 0.5$, $Re_{t,\infty} = 10^{-2}$, $k_\infty/u_\infty^2 = t_{kinf}$).



a) Pressure coefficient (C_p)

b) Skin-friction coefficient (C_f)



c) Free-stream dependency of TNT $k-\omega$ variant

d) Grid dependency of TNT $k-\omega$ variant

Fig. 4 Pressure and skin-friction distribution for RAE2822 airfoil, case 9 with $k-\omega$ model ($M_\infty = 0.73$, $Re_\infty = 6.5 \cdot 10^6$, $\alpha = 2.8^\circ$, $Re_{t,\infty} = 10^{-2}$, $k_\infty/u_\infty^2 = 10^{-6}$).